

# BEHAVIOUR OF YARN INTERACTED WITH HIGH-SPEED OBJECT UNDER SIDEWAYS-CONSTRAINT

**Dang Vu Hung, Joris Degrieck\*, Lievan Van Langenhove & Paul Kiekens**

Department of Textiles

\*Department of Mechanical Production and Construction

Ghent University

Technologiepark 9, 9052 Zwijnaarde, Belgium

E-mail: vuhung.dang@rug.ac.be

## **Abstract**

*This paper presents an investigation of the dynamic behaviour of a yarn in an interaction with a high-speed object, for the lower warp sheet during the weaving process. The yarn movement on the object can be described in four stages from non-contact, contact, drop-off and withdrawal. A model is developed to predict this interaction, taking into account several factors such as yarn length, yarn tension, object speed, object orientation and object profile. A comparison of theoretical predictions and experimental measurements for different yarns indicates a good agreement. The theoretical model can be used to optimise the object profile in order to reduce the interactive yarn tension and to avoid any yarn damage.*

## **Introduction**

On most modern looms, during the passage from the warp beam to the cloth fell the warp yarns are in contact with machine elements at several points such as drop wires, heald eyes, reed dents. During shedding and the insertion process, the warp yarns at the lower shed interact with some objects, which are driven by the slay. These objects are of several types: rapier hooks, relay nozzles, opening levers of positive rapier loom etc [5]. As a result of this interaction, yarn tension rises and the yarn itself may be damaged in severe cases.

The understanding and modeling of the interaction process is of high importance for the weaving industry. Knowledge of the interaction phenomena allows determination of yarn tension and strain, taking place at every moment during the interaction. Based on the obtained results and using the model, damage to the warp yarn caused by those objects, can be minimised in a later phase.

Regarding this kind of interactions, Vickers et al. [16] recently studied the yarn-to-object surface friction, where a stationary object with an elliptical profile was used and where yarn displacements were determined by means of digital imaging techniques. In the field of the sewing process Stylios [14] pointed out that an optimum design of the point of the needle is of paramount importance to decrease the needle penetration force, when the needle is pushed through the fabric. Lomov [10] further developed the model proposed by Stylios for the study of the interaction of a woven fabric and a needle, taking into account mechanical properties of the yarn in weft and warp direction.

This paper presents a mathematical model, which describes the simulation of the interaction between yarn and object under sideways constraint by the reed in the lower warp sheet during the weaving process. The described model will then be validated using different yarns and a relatively large object, the profile of which is clearly defined.

## **Experimental set-up**

### **Test materials**

The properties of the yarns used in this study are summarized in Table 1:

**Table 1:** Properties of yarns used in experiments

Yarn type	Linear density, tex	Tenacity, cN/tex	Elongation, %	Initial Modulus, cN/tex
Cotton (Co)	100	13.4	2.7	538.3
Wool (Wo)	60	19.3	24.1	208.4
Polyamide (PA)	18	37.4	30.8	226.4

All yarn samples were conditioned in a testing atmosphere of  $20 \pm 1^\circ\text{C}$  and  $65 \pm 4\%$  r.h. for at least one day.

The object sideways shape is generally defined as consisting of two parts: a curved and straight profile, as shown in Figure 1. The curved profile of object can be linear or non-linear, and  $r$ ,  $h$  are the object radius and the height of the curved profile.

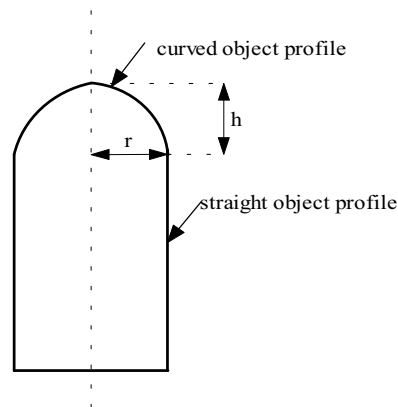


**Figure 1:** general shape of the sideways-object profile

### Testing apparatus

To simulate the interaction process at the lower warp sheet, a testing apparatus was constructed which has already been described elsewhere [5].

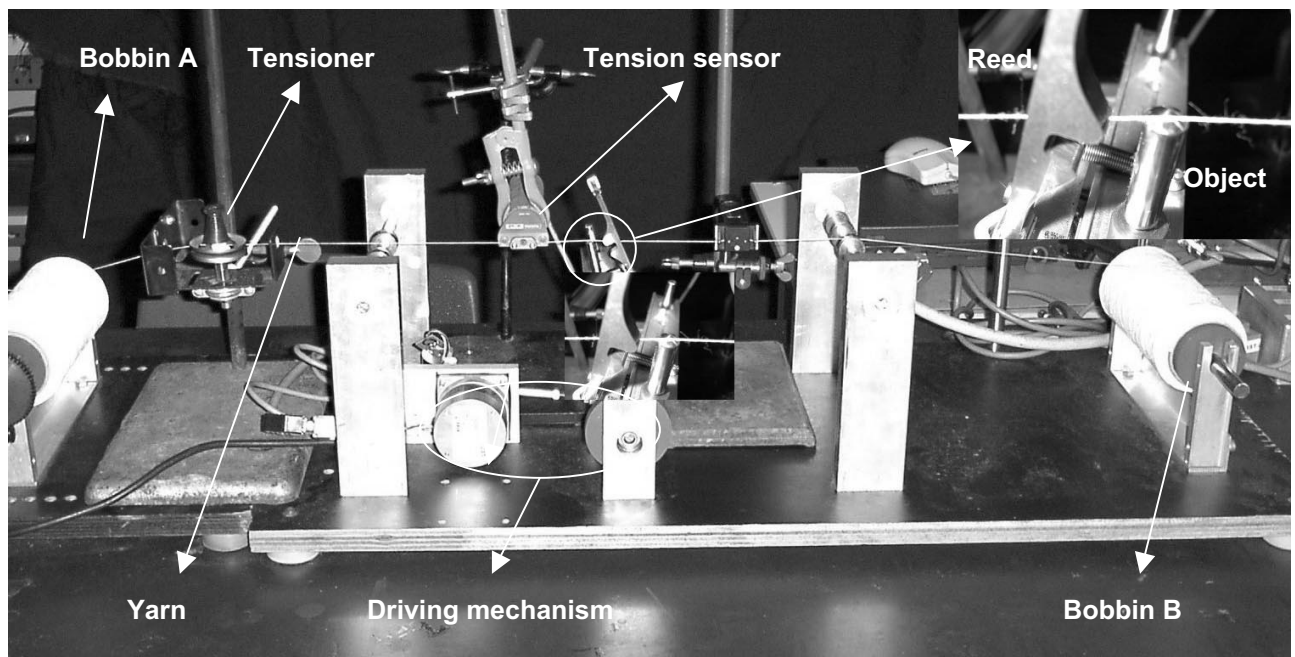


**Figure 2:** Testing apparatus

In this apparatus, a piece of reed (cut from the real reed on a loom) was placed firmly on the slay; it can be set at a certain angle relative to the object.

### Tension measurements

The yarn tension measurement system is shown in Figure 3. A signal from a tension sensor (IRO dynamic tensiometer, range 0-200 cN) is stored onto a laptop Pentium 100MHz via a channel box and data acquisition card (DAQCard-AI-16E-4, National Instruments). The sampling rate of the tension signal is chosen as function of the speed of the moving object. Precautions were taken for eliminating the effect of vibrations of the apparatus.

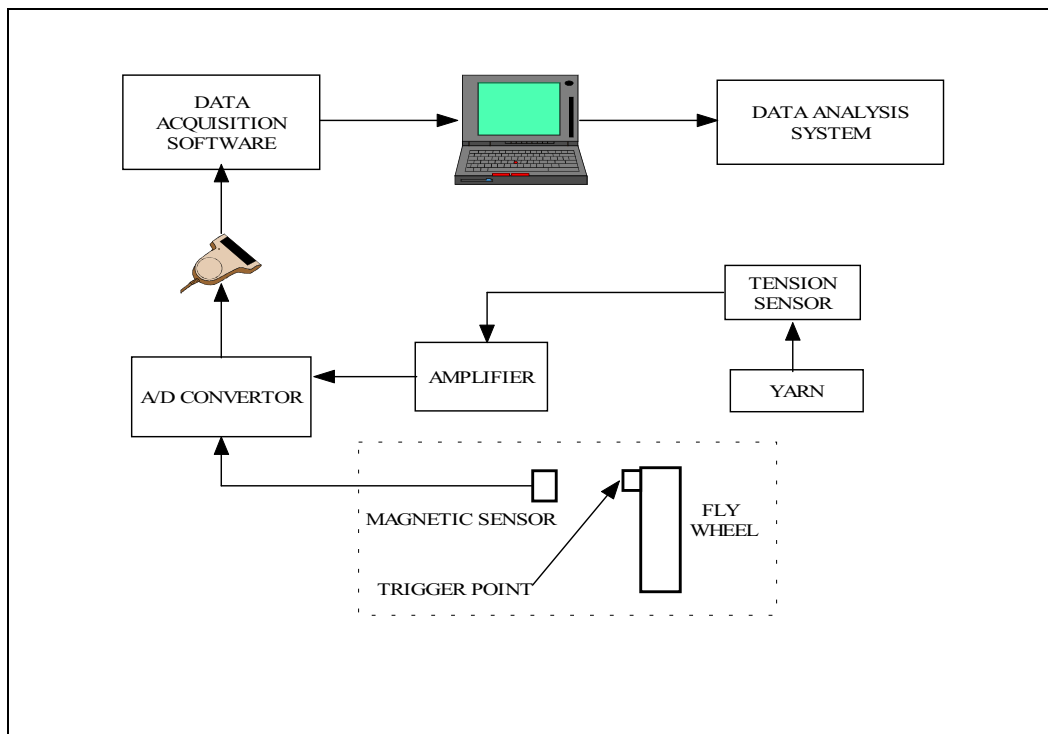


**Figure 3:** Yarn tension measurement system

Before the start of each test, a calibration of the amplifier was performed for each type of yarn. The calibration was determined by applying a known weight and by recording the sensor output voltage.

The tension sensor was positioned on the starting side of the object movement. Referring to the well-known capstan equation it hence measures a higher tension in the upward movement and a lower tension in the downward movement.

Data collection of yarn tension involved two steps, which were repeated for each experiment performed. In the first step, the data were collected while the apparatus operated, but with the absence of object. In this way the data from this step comprise the yarn pre-tension, noise and apparatus vibration. The second step involved data collection including the interaction of the object and the reed. The difference between both signals resulted in the yarn tension rise as a function of time. The signals were taken as the mean from several measurements for further noise reduction.

### Image recording

It was desired to record the motion of the yarn caused by the interaction with the object by using a high-speed camera system (Kodak system). This camera has three recording rates: 250, 500, 1000 frames per second. The high-speed camera captures images and stores them internally. Based on the maximum device speed of 240 rpm, the recording rate of 500 frames per second was chosen. This rate was found to be fast enough to give sufficient image quality detail of the yarn movement. By slow-motion replay, images were recorded on a video recorder.

## Theoretical development

### Qualitative description of the interaction

The action of the object has the following effects on the warp yarn. Initially, the yarn is pushed upward by the object, thus increasing strain in the yarn. At the same time, the object slides on the yarn. The yarn does not start sliding sideways from the object tip until some conditions are met. If at some instant the resulting yarn strain exceeds its breaking strain, then the yarn will break. If not so, yarn tension increase may still be large enough to give some damage to the yarn, or more severely, penetrate into the yarn. The sideways movement of the yarn is constrained by the presence of the reed, which imposes higher pressure on the yarn in the interaction side. After yarn flipping off has occurred friction will exist between yarn and object/reed. The actual effect of this interaction is largely dependent on the yarn structure, initial yarn tension, object and reed surface characteristics as well as object profile.

### Interaction analysis

The whole interaction between the yarn and the object or reed can be described in terms of the measured yarn tension. In the proposed model, the following assumptions were made:

- 1) the yarn cross section is circular and remains unchanged during the interaction;
- 2) the total normal force of the yarn on the object surface is always perpendicular to the original yarn line; with the geometric parameters used, this gives only a very small error,
- 3) the initial position of the yarn on the object is assumed to be slightly eccentric, which corresponds with reality,
- 4) as axial yarn velocity on real looms is very small, compared to object velocity, it is supposed to be zero,
- 5) yarn deformation is linear following Hooke's law.

Figure 4 gives a schematic view of the global geometry used in the model:

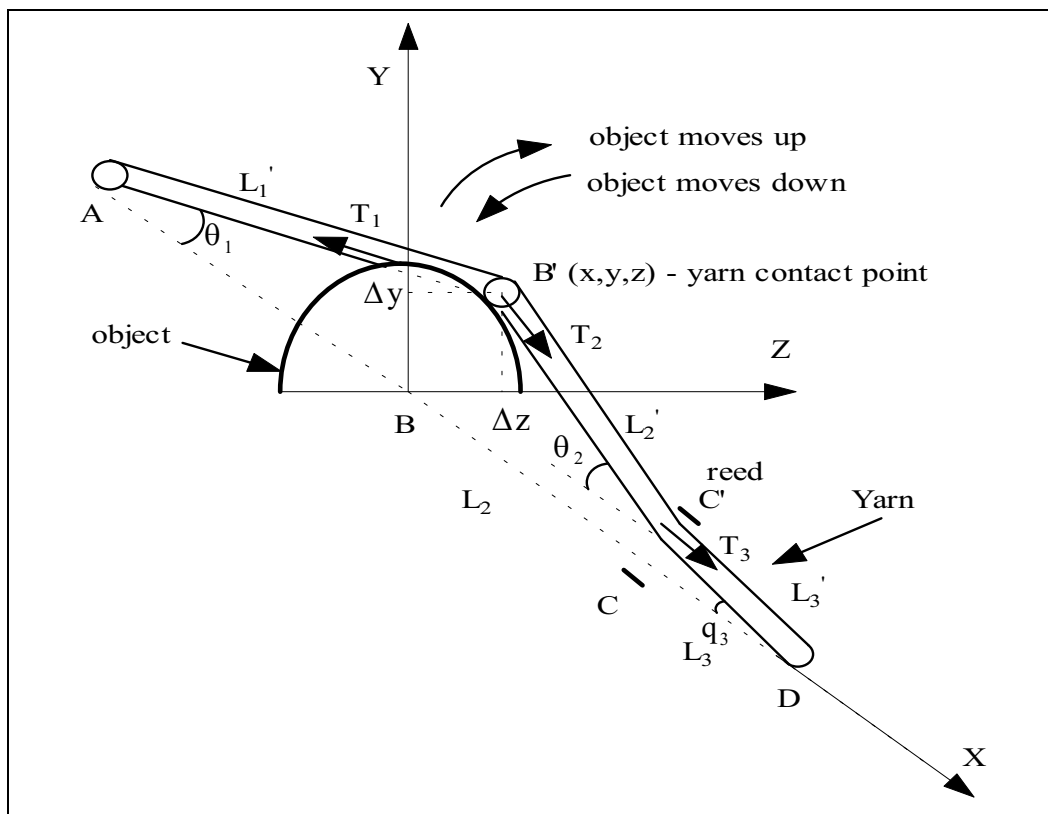


Figure 4: Sketch showing the geometry of the yarn-to-object surface

As the object rises, the yarn comes into contact with the object. Generally at this moment, there is no contact between yarn and reed yet. The yarn, which may be considered as an elastic string of initial length  $L_0$  (ABCD) between two clamps, is extended to a new length AB'C'D, thus dividing the yarn into two homogeneous strings AB' and B'D. The tangential component of the movement i.e., parallel to the original yarn, will create a frictional force, which will produce different yarn tensions on both sides of the object. The yarn tensions will increase until they exceed the frictional resistance. From that moment the object will start to slide over the yarn. If the deformation of the yarn is supposed to be linear, then the Hooke's law can be applied:

$$T = T_0 + \varepsilon_t E \quad (1)$$

In this equation:  $E$  is the yarn initial modulus,  $T$  is the tension that would occur if friction is neglected and  $\varepsilon_t$  is the average yarn extension.

When the yarn is deflected sideways it slides down along the edge of the object profile. At the moment that the yarn reaches the edge of the reed, its movement in the  $z$  direction is constrained. From this point, it is possible to treat the yarn as consisting of three homogeneous strings AB', B'C' and C'D. The average extension of all yarn segments can be calculated as:

$$\varepsilon_t = \frac{\sqrt{L_1^2 + \Delta y_1^2 + \Delta z_1^2} + \sqrt{L_2^2 + (\Delta y_1 - \Delta y_2)^2 + (\Delta z_1 - \Delta z_2)^2} + \sqrt{L_3^2 + \Delta y_2^2 + \Delta z_2^2} - L_0}{L_0} \quad (2)$$

in this formula:

$\Delta y_1, \Delta z_1$  and  $\Delta y_2, \Delta z_2$  are the deflection of yarn contact points B' and C' in the Y and Z direction, with  $\Delta z_1 \leq r - z_{10}$ ,  $\Delta z_2 \leq \xi$  with  $z_{10}$  and  $\xi$  are the initial position of the yarn on the object and distance from the original yarn line to the reed edge respectively in the Z direction;

$L_1, L_2, L_3$  are the length of yarn segments AB, BC, CD which are time-dependent as the object and the reed move during the interaction.

These can be used as the boundary conditions for the yarn movement on the object surface.

The yarn tensions  $T_1, T_2$  and  $T_3$  in the three yarn segments AB', B'C' and C'D can be formulated similar to those described in [5]. Here we have:

$$T_1 = \frac{TL_0 e^{\pm\mu_1\theta_t} e^{\pm\mu_2\theta_r}}{L_1 e^{\pm\mu_1\theta_t} e^{\pm\mu_2\theta_r} + L_2 e^{\pm\mu_2\theta_r} + L_3} \quad (3)$$

$$T_2 = \frac{TL_0 e^{\pm\mu_2\theta_r}}{L_1 e^{\pm\mu_1\theta_t} e^{\pm\mu_2\theta_r} + L_2 e^{\pm\mu_2\theta_r} + L_3} \quad (4)$$

$$T_3 = \frac{TL_0}{L_1 e^{\pm\mu_1\theta_t} e^{\pm\mu_2\theta_r} + L_2 e^{\pm\mu_2\theta_r} + L_3} \quad (5)$$

where  $\mu_1$  is the friction coefficient between yarn and object,  $\mu_2$  is the friction coefficient between yarn and reed,  $\theta_t$  ( $\theta_t = \theta_1 + \theta_2$ ) and  $\theta_r$  ( $\theta_r = \theta_2 + \theta_3$ ) are the contact angle of the yarn around the object and against the reed respectively; '+' if the object moves up, and '-' if the object moves down.

The frictional forces between yarn and object surface and between yarn and reed edge can be drawn from the values of  $T_1, T_2$  and  $T_3$ .

In this analysis, it is very important to note that object shape and its surface characteristics play a major role in determining the yarn movement. The conditions at which the yarn sticks or slips down

over the surface, are based on a dynamic force balance at each possible yarn-to-surface contact position.

We now consider the yarn movement in the Plane Y-Z as given in Figure 5:

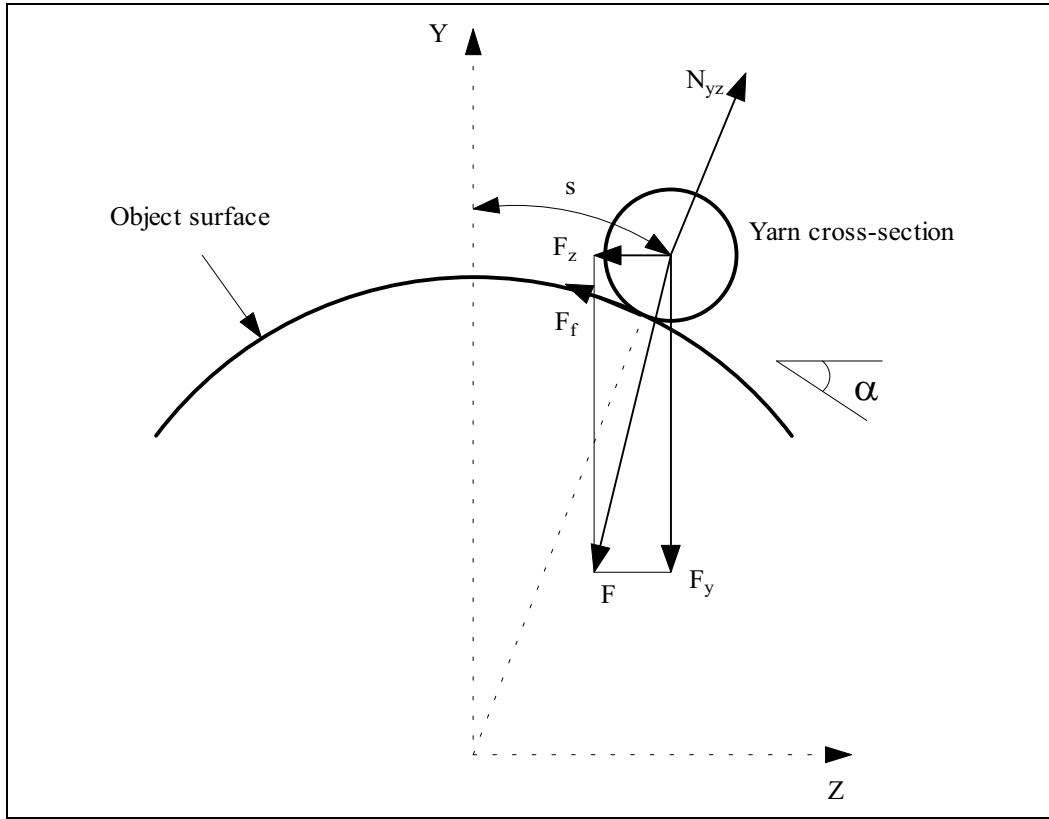


Figure 5: Forces acting on a yarn on the side of the object

The cross-sectional element of the yarn is acted upon by several forces, where  $F$  is the resultant force in the Y-Z plane of  $T_1$  and  $T_2$ ,  $N_{yz}$  is the normal force and  $F_f$  is the frictional force of the yarn against the object surface. If  $\alpha$  is a tangential angle of the yarn with respect to the object at the point of contact,  $\alpha$  can be determined:

$$\alpha = \tan^{-1}\left(\frac{dy}{dz}\right)$$

in which  $y=f(z)$  is the equation of the object profile.

The displacement force ( $F_d$ ) acting upon the yarn in the tangential direction and the normal force ( $N_{yz}$ ) are obtained as:

$$F_d = F_y \sin \alpha - F_z \cos \alpha \quad (6)$$

$$N_{yz} = F_y \cos \alpha + F_z \sin \alpha \quad (7)$$

where  $F_y$  and  $F_z$  can be calculated from the tensions  $T_1$ ,  $T_2$  and  $T_3$ .

According to the law of Coulomb [6] the frictional force created during yarn movement on the object surface in this plane is dependent on the relative velocity of the yarn. The following must be complied:

$$F_f = \mu \frac{v_{yz}}{\sqrt{v_x^2 + v_{yz}^2}} |N| \quad (8)$$

where  $v_x, v_{yz}$  is the relative velocity of the yarn in the x direction and in the Y-Z plane respectively,

$N = \sqrt{N_x^2 + N_{yz}^2}$  is the total normal force, where  $N_x$  is the normal force in the x direction.

The yarn is initialized sideways if the following condition is fulfilled:

$$|F_d| > F_f \quad (9)$$

The yarn motion along the object profile is complicated because the absolute motion of the yarn is the combination of two motions: the relative motion of the yarn to the object surface and the following motion with the object.

$$\vec{v}_{yz} = \vec{v}_e + \vec{v}_r \quad (10)$$

Generally, this absolute motion can be expressed by using the Lagrangian equation of second kind:

$$\frac{d}{dt} \left( \frac{\partial K}{\partial \dot{q}} \right) - \frac{\partial K}{\partial q} + \frac{\partial \Pi}{\partial q} + \frac{\partial R}{\partial \dot{q}} = 0 \quad (11)$$

where  $K$  is the kinetic energy,  $\Pi$  is the potential energy,  $R$  is the dissipative energy,  $q$  is the general coordinate and  $\dot{q}$  is the derivative of  $q$  according to time. In this case, we select  $q = s$  (see Figure 5). The relations describing the kinetic energy can be approximated by:

$$K = \frac{1}{2} m_1 v_1^2 + \frac{1}{2} m_2 v_2^2 + \frac{1}{2} m_3 v_3^2 + \frac{1}{2} I_1 \dot{\theta}_1^2 + \frac{1}{2} I_2 \dot{\theta}_2^2 + \frac{1}{2} I_3 \dot{\theta}_3^2 \quad (12)$$

where  $m_1, m_2$  and  $m_3$  are the weights of yarn strings AB', B'C' and C'D respectively, with their middle point of each segment (regarded as a centre of mass) moving at the velocity of  $v_1, v_2$  and  $v_3$ ;  $I_1, I_2$  and  $I_3$  are the moment of inertia of these three beams.

Taking into account of interaction geometry, the kinetic energy is derived:

$$K = \frac{1}{2} m v_{yz}^2 \quad (13)$$

where  $m = \frac{5}{12} m_1 + \frac{1}{48} (27m_2 + 11m_3) \sin^2 \alpha + \frac{1}{4} m_2 \cos^2 \alpha$

The potential energy is obtained as:

$$\Pi = -(F_d - F_f) s + \text{const} \quad (14)$$

The dissipative energy or the energy dissipated by impressing between the yarn surface and the object surface due to elasticity variation can be determined by the following formula:

$$R = \frac{1}{2} \eta \dot{s}^2 \quad (15)$$

with  $\eta$  is the yarn damping coefficient.

By taking a derivative of these relations with respect to time and general coordinate  $s$  and substituting into the Lagrangian equation, we obtain a differential equation of the second order:

$$m \ddot{s} + \eta \dot{s} = F_d - F_f \quad (16)$$

Equation (16) expresses the motion of the yarn when sliding down the profile of the object in the Y-Z plane. This equation can be integrated in time by using the Runge-Kutta method, such as it is available in commercial mathematical software.

It must be noted that the yarn movement on the curved profile differs from that on the straight profile. When the yarn arrives at the intersection point between these two curves, the yarn acceleration is very high but still finite. The yarn drops off very quickly and vibrates. The vibration frequency depends very much on yarn tension, yarn starting acceleration, yarn weight, yarn damping coefficient and frictional forces generated on the object surface and at the reed edge. This frequency can be approximated by:

$$\omega = \frac{1}{2\pi} \sqrt{\frac{F_y}{m} \frac{L_1 + L_2}{L_1 L_2}} \quad (17)$$

After the object and the reed have completed their upward movement, they retract towards their initial position in the downward path. The initial interaction between the yarn and the object on the straight profile of the object is purely frictional. Again at the intersection point of the two curves, the yarn withdraws very fast like a “flip-up”. However, the vibration frequency is now less than that at the drop-off.

This is the end of one interaction cycle between yarn and object.

## Results and discussion

The parameters used in the experiment are: the initial tension  $T_0 = 0.8 \text{ N}$ ;  $\mu = 0.15$  for cotton 100 tex,  $\mu = 0.1$  for PA 18 tex and  $\mu = 0.12$  for wool 60 tex; these friction coefficients are dependent on yarn basic tension, contact angle and relative velocity between yarn and object [4]. The initial yarn length  $L_0 = 0.15 \text{ m}$ , the object radius = 0.002 m (a larger object rather than those generally employed in the real loom was used in order to demonstrate more clearly the behaviour of the yarn during the interaction), and the object curved profile  $y = 0.7z$ .

Table 2 shows the predictions of the drop-off moment by the model:

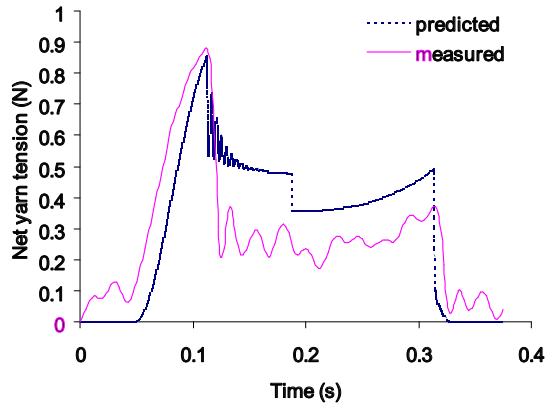
**Table 2:** predicted v.s measured drop-off moment given by the high speed video camera

Yarn type	Device speed (rpm)	Drop-off moment (s)	
		Measured	Predicted
Wool 60 tex	132	0.080	0.078
Wool 60 tex	168	0.062	0.062
Wool 60 tex	240	0.044	0.042
Cotton 100 tex	168	0.062	0.062
PA 18 tex	168	0.062	0.062

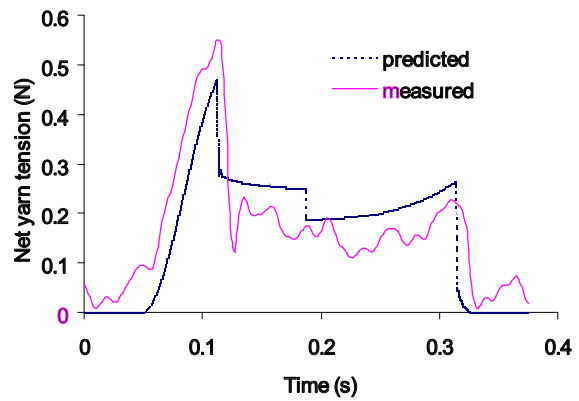
From Table 2 it can be seen that the drop-off moment of the yarn is independent of yarn fineness. It is probable that the yarn movement occurs as a series of static equilibrium positions. At every equilibrium position, the yarn velocity becomes zero. Furthermore, the device speed also has no influence on the drop-off moment, as the fraction of time the yarn moves on the curved profile is proportional to the device speed (0.080s/0.062s/0.044s versus 132rpm/168rpm/240rpm).

The model appears to be a good predictor of yarn tension increase experienced during the interaction. Figure 6 compares the results obtained for the different yarn types.

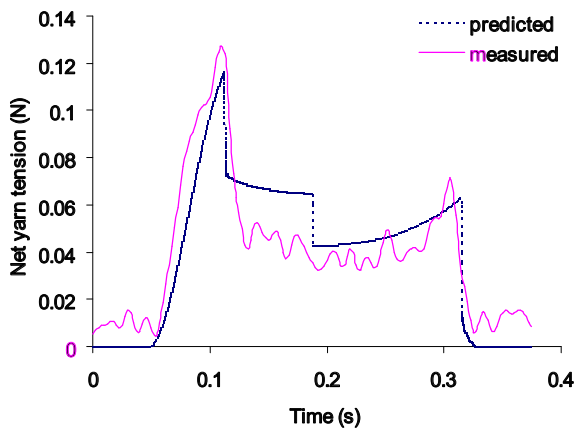




a. Cotton 100 tex



b. Wool 60 tex



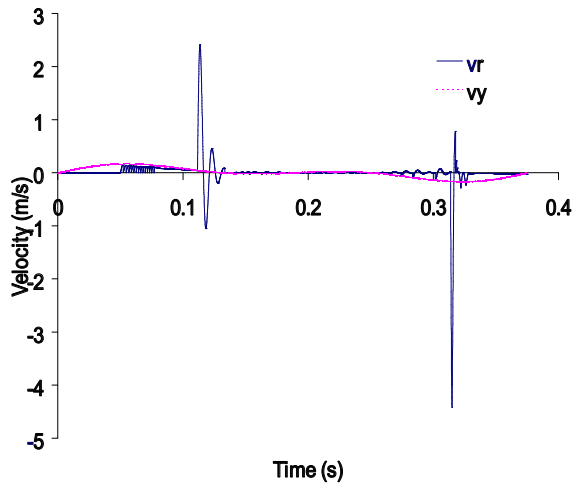
a. PA 18 tex

**Figure 6:** predicted v.s measured yarn tension increase (apparatus speed: 168 rpm)

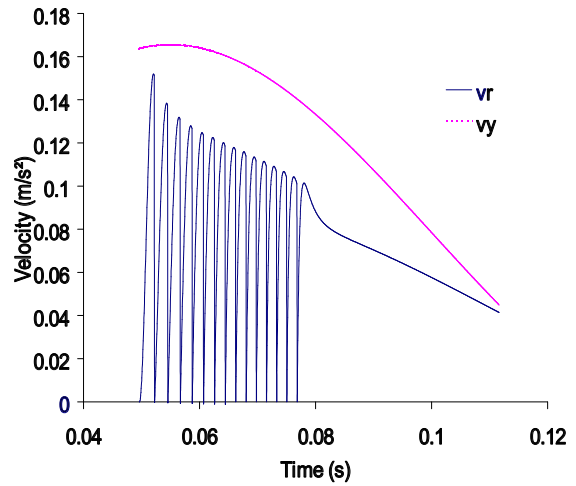
The measured net yarn tension histories are estimated very well, taking into account the differences in scale for the different yarns. For shorter yarn lengths, the prediction becomes less accurate, which can be due to the paid-off length of the yarn at the tensioner. The correlation coefficient is 82%, 82% and 87% for the case of cotton 100 tex, wool 60 tex and PA 18 tex respectively.

The tension peak appears at the drop-off moment. Before dropping off, Figure 6 shows that the tension curve is quite smooth at this stage. It also means that the yarn moves persistently down along the object curved profile. The yarn drop-off generates transverse vibration, which occurs in a very short time or for a while depending on the force level, yarn starting acceleration and yarn damping coefficient. In addition, it is expected to observe a jump of the yarn tension at the transition point between the upward and downward movement. However, the mechanical and circuit vibration imparted on the tension measurement distorts a bit this scenario.

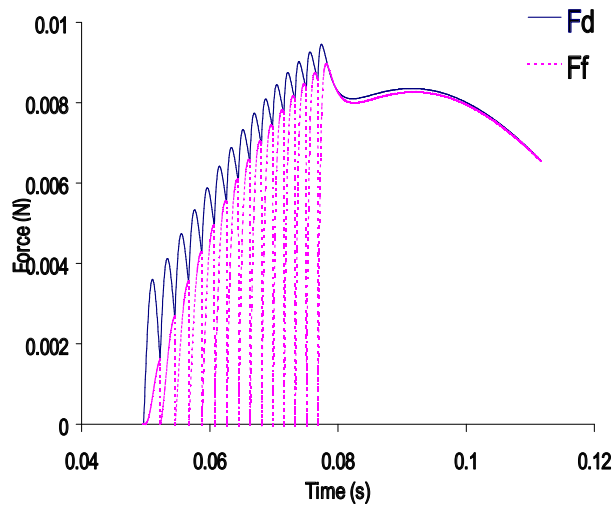
The other interesting parameters of the interaction are the relative velocity, displacement force and frictional force of the yarn at the sideways movement. Figure 5 shows the results conducted for PA 18 tex:



a. Sideways relative velocity of yarn v.s object tip velocity in the Y direction



b. Sideways relative velocity of yarn v.s object tip velocity in the Y direction (on the curved profile of the object in the upward movement)



a. Displacement force v.s frictional force on the curved profile of the object in the upward movement

**Figure 7:** Yarn velocity and forces acting on the yarn (PA 18 tex) at the sideways movement

It is found that the theoretical and experimental results are favourably correlated. To investigate the effects of varying object profile, pre-tension values, pre-position of yarn on object, yarn length used in the interaction etc., we just make use of computer simulations.

## Conclusions

In this study, we present a numerical approach to model the yarn-object interaction under a reed-sideways constraint as occurs at the lower warp sheet during the weaving process. Comparisons with experimental data confirm the accuracy of the present model. Factors influencing the yarn tension mainly include mechanical properties of yarn, yarn length, object thickness, object surface characteristics, object profile, contact length, and machine speed. The model suggests that the slope at any point on the profile curve of the object is one of the most important factors in the interaction. A smaller slope results in a lower tension variation in the yarn. Using the model for optimising the yarn

tension during interaction between yarn and object will help in conceiving an ideal object, by which eventually no yarns at all are disturbed. This model can also be extended to apply in real loom situations, taking into account all related constraints in the lower warp sheet.

## References

1. Atkinson, Doney A.N., *Optimum Experimental Designs*, Oxford Science Press (1992)
2. Baird M. E, *Friction Properties of Nylon Yarn and Their Relation to the Function of Textile Objects*, J. Textile Inst., Vol 46 (1955) pp 101-111
3. Bajpai A.C. et al., *Numerical Methods for Engineers and Scientists*, John Wiley & Sons (1978)
4. Dang V.H. et al., *Frictional model of yarns running against objects*, Proceedings of 2<sup>nd</sup> International Conference "Novelties in Weaving Research and Technology", Liberec, Czech Republic (1998)
5. Dang V.H. et al., *Numerical Simulation of the Yarn-Object Interaction*, accepted for Textile Res. J
6. Degrieck J., *Kinematics and dynamics of machines*, Universiteit Gent (2000)
7. Gupta. B. S and El Mogahzy, *Friction in Fibrous Materials, Part 1: Structural Model*, Textile Res. J, Vol 61 (1991) pp 547-555
8. Gupta. B. S and El Mogahzy, *Friction in Fibrous Materials, Part 2: Experimental Study of the Effect of Structural and Morphological Factors*, Textile Res. J, Vol 63 (1993)pp 219-230
9. Howell, H.G., and Mazur, J., *Amontons Law and Fibre Friction*, J. Textile Inst., Vol 44, (1955) pp 41-58
10. Lomov.L, *A Predictive Model for the Penetration Force of a Woven Fabric By a Needle*, International Journal of Clothing Science and Technology, Vol 10 No 2 (1998) pp 91-103
11. Lyne D.G, *The Dynamic Friction Between Cellulose Acetate and a Cylindrical Metal Surface*, J. Textile Inst., Vol 46 (1955) pp 112-118
12. Olsen. J. S, *Frictional Behaviour of Textile Yarns*, Textile Res. J., Vol 39 (1969) pp 31-37
13. Rubenstein C., *The Friction of a Yarn Lapping a Cylinder*, J. Textile Inst., Vol 49 (1958) pp 181-191
14. Stylos.G, *An Investigation of the Penetration Force Profile of the Sewing Machine Needle Point*, J.Text.Inst., Vol 86 (1995)
15. Vangheluwe.L, *Influence of Strain Rate and Yarn Number on Tensile Test Results*, Textile Res. J, Vol 62 (1992) pp 586-589
16. Vickers A. D et al., *Analysing Yarn-to-Surface Friction with Data Acquisition and Digital Imaging Techniques*, Textile Res. J, Vol 70 (2000) pp 36-43